Generalized EEG-Based Drowsiness Prediction System by Using a Self-Organizing Neural Fuzzy System

Fu-Chang Lin, Li-Wei Ko, *Member, IEEE*, Chun-Hsiang Chuang, Tung-Ping Su, and Chin-Teng Lin, *Fellow, IEEE*

***Abstract*—A generalized EEG-based Neural Fuzzy system to predict driver's drowsiness was proposed in this study. Driver's drowsy state monitoring system has been implicated as a causal factor for the safety driving issue, especially when the driver fell asleep or distracted in driving. However, the difficulties in developing such a system are lack of significant index for detecting the driver's drowsy state in real-time and the interference of the complicated noise in a realistic and dynamic driving environment. In our past studies, we found that the electroencephalogram (EEG) power spectrum changes were highly correlated with the driver's behavior performance especially the occipital component. Different from presented subject-dependent drowsy state monitor systems, whose system performance may decrease rapidly when different subject applies with the drowsiness detection model constructed by others, in this study, we proposed a generalized EEG-based Self-organizing Neural Fuzzy system to monitor and predict the driver's drowsy state with the occipital area. Two drowsiness prediction models, subject-dependent and generalized cross-subject predictors, were investigated in this study for system performance analysis. Correlation coefficients and root mean square errors are showed as the experimental results and interpreted the performances of the proposed system significantly better than using other traditional Neural Networks (p-value <0.038). Besides, the proposed EEG-based Self-organizing Neural Fuzzy system can be generalized and applied in the subjects' independent sessions. This unique advantage can be widely used in the real-life applications.**

***Index Terms*—Drowsiness, drowsy state monitoring, electroencephalogram (EEG), neural fuzzy system, prediction.**

Manuscript received May 21, 2011; revised October 18, 2011; accepted December 16, 2011. Date of publication February 07, 2012; date of current version August 24, 2012. This work was supported in part by the UST-UCSD International Center of Excellence in Advanced Bio-engineering sponsored by the Taiwan National Science Council I-RiCE Program under Grant NSC-100-2911-I-009-101, in part by the Aiming for the Top University Plan of National Chiao Tung University, the Ministry of Education, Taiwan, under Contract 100W963, in part by the VGHUST Joint Research Program, Tsou's Foundation, Taiwan, under Contract VGHUST100-G5-2-3, and in part by the National Science Council, Taiwan, under Contract 100-2628-E-009-027-MY3. Research was also sponsored in part by the Army Research Laboratory and was accomplished under Cooperative Agreement Number W911NF-10-2-0022. L. W. Ko and F. C. Lin provide the equal contribution of this work. This paper was recommended by Associate Editor B. Shi.

F.-C. Lin, C.-H. Chuang, and C.-T. Lin are with the Brain Research Center and the Department of Electrical Engineering, National Chiao Tung University, Hsinchu 30010, Taiwan (e-mail: Fu-Chang.Lin@synopsys.com; cch.chuang@gmail.com; ctlin@ma).

L.-W. Ko is with the Department of Biological Science and Technology, and Brain Research Center, National Chiao Tung University, Hsinchu 30010, Taiwan (e-mail: lwko@mail.nctu.edu.tw).

T.-P. Su is with Department of Psychiatry, Taipei Veterans General Hospital, Taipei, Taiwan (e-mail: tpsu@vghtpe.gov.tw).

Color versions of one or more of the figures in this paper are available online at http://ieeexplore.ieee.org.

Digital Object Identifier 10.1109/TCSI.2012.2185290

I. Introduction

THE development of a human drowsy state monitoring system for drivers has become a major focus in the field of safety driving and accident prevention because drivers' fatigue has been implicated as a causal factor in many car accidents. The 2009 Sleep Report of National Sleep Foundation (NSF) in America poll shows that 1% or as many as 1.9 million drivers have had a car crash or a near miss due to drowsiness in the past year. Even more surprising, 54% of drivers (105 million) have driven while drowsy at least once in the past year, and 28% (54 million) do so at least once per month [1]. Hence, the development of countermeasures against a serious threat to driver safety is an urgent necessity. Such an in-vehicle system requires the capabilities of continuously monitoring the arousal state of the driver, accurately predicting the potential impact on the driving performance, and delivering a timely warning before dropping asleep.

Many studies related to drowsy state monitoring and detection technologies have been developed during the last decade. Kozak *et al.* [2] and Rimini-Doering *et al.* [3] proposed a similar lane-departure warning system via tracking lane marks by camera systems for the assisted drivers. A different approach is to monitor the activities of the drivers themselves such as yawning, head positions, or eye blink duration by using optical sensors or video cameras [4], [5]. However, image- or video-based techniques are sensitive to external weather conditions, e.g., rain or snow, and are easily influenced by the driver's posture inside the car. McGregor *et al.* [6] introduced a technique to monitor the drivers' physiological states by directly acquiring and analyzing subject's heart-rate variability (HRV) and electrooculography (EOG) [7] signal, which can overcome the system disadvantages mentioned above. Nevertheless, the minute-length scale of HRV and EOG analyses limit the monitoring system to a low-temporal-resolution output.

Recently, numbers of studies in neural engineering are devoted to explore the informative index of scalp EEG activities engaging with the particular cognitive task. With the high-temporal-resolution of the sampling rate and the portability of the hardware, the EEG has been shown as a promising approach to effectively assess the physiological states. Review of the existing studies related to the low performance, fatigue, or drowsiness [8]–[26], the changes in EEG power spectrum are regarded as the robust index for the change of the cognitive state. Beatty *et al.* [8] demonstrated the phenomenon of

increasing occipital theta (4–7 Hz) power when the radar operators were less vigilant. Huang *et al.* [9] demonstrated tonic EEG power increase in low-frequency bands in the occipital cortex during high-error periods in a continuous visual tracking task, and they also showed similar tonic EEG power increase in low-frequency bands in the occipital cortex in simulated driving experiments [10]. In addition, Lin *et al.* [11] have shown the high correlation between alpha (8–11 Hz) and theta (4–7 Hz) band power and driving error, which is defined as the mean deviation from lane center in each moving window in the virtual-reality (VR) environment. Besides, the research [12] showed that changes in EEG spectra in the theta band and alpha band reflect changes in the drowsy state and memory performance. Other studies also showed that the EEG power spectra in the theta [13] and/or alpha [14] bands are associated with drowsiness, and EEG power spectrum has largely linearly related to subject's driving performance. According to these fundamental findings, several algorithms and systems are proposed [11], [15]–[22]. Our research [11], [15]–[19] have demonstrated an automatic drowsy state prediction system with EEG power spectra by constructing a linear regression model. In [17], an independent component analysis-based (ICA-based) Fuzzy Neural Networks was proposed based on the independent sources instead of the scalp EEG activities. Moreover, the comparison of three neural networks based monitoring system was shown in [23]. The performance could reach a low prediction error across subjects while using the occipital component. Subasi *et al.* [20], Kiymik *et al.*, [21] and Vuckovic *et al.* [22] also successfully demonstrated an automatic recognition algorithm to classify alertness level with the combination of EEG power bands among 1–30 Hz.

However, most of the proposed models are a subject-dependent system, i.e., the parameters of the system are not a generalization solution for each individual. Consequently, the performance might be unreliable. Hence, based on the discoveries in the researches mentioned above, this study proposes a generalized EEG-based Self-organizing Neural Fuzzy Inference Network (SONFIN) system to monitor the occipital theta- and alpha-band power and further predict the driver's reaction time (RT) to an unexpected event. Two kinds of drowsiness prediction models, the subject-dependent and generalized cross-subject ones, were investigated. The system performances of SOFIN are compared with three benchmark systems including the Multi-Layer Perceptron Neural Network (MLPNN), the Radial Basis Function Neural Network (RBFNN) and Support Vector Regression (SVR) with Radial Basis kernel. Experimental results indicate that the proposed system performs better than other systems in correlation analysis and prediction error especially for the cross-subject model. It advantages the development of in-vehicle protocol to the real-life applications for the publics.

II. Experimental Setup

A. Virtual Reality (VR)-Based Dynamic Driving Simulator

The experiments in this study used a VR-based highway-driving environment shown in Fig. 1. This simulator was developed in our previous studies [17], [18] to investigate the changes of the driver's drowsy state during long-term monotonous driving at a fix speed of 100 km/hr. The experimental environment includes a 3-D surrounding view projected by seven projectors, and a real car mounted on a six-degree of freedom Stewart platform [22]–[25], as Fig. 1(a) and (b) shown. All scenes move depending on the displacement of the car and the subjects maneuvering of the wheel during the driving experiments, making drivers feel like they are driving a real car on a real road.

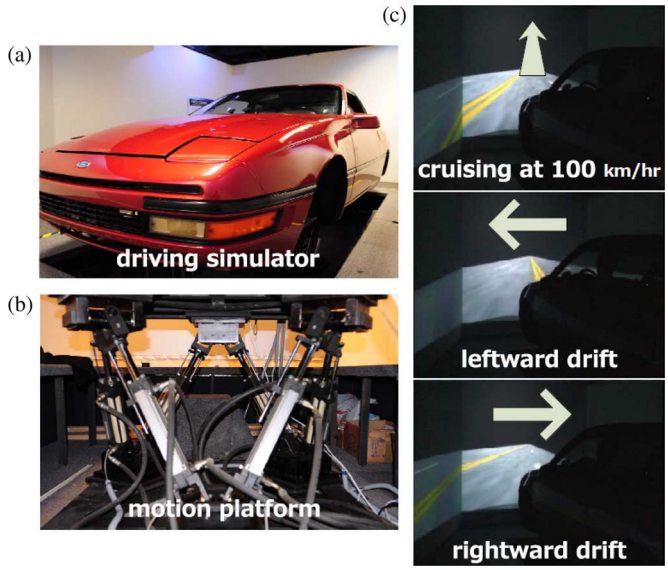

Fig. 1. VR-based highway driving environment. (a) Driving simulator, (b) six degree-of-freedom motion platform, and (c) illustration of driving task, adapted from [9].

B. Event-Related Lane-Departure Experiment

This study implemented the event-related lane-departure paradigm [10] on the driving simulator. The simulator automatically and randomly drifts the car away from the center of the cruising lane as shown on Fig. 1(c). The subjects were instructed to keep the car in the third lane using the steering wheel whenever the occurrence of a lane-departure event. During an hour-long experiment, this unexciting and monotonous task easily makes drivers fall asleep. Each lane-departure event (or "trial") captured the acquired EEG data, deviation distance, and time latency for analysis. Three important time points (see Fig. 2(a)) in this experiment were recorded to determine the driving trajectory [10]: (1) deviation onset—the time at which the car starts to drift away from the cruising lane, (2) response onset—the time at which the subject starts responding to the car-drifting event, and (3) response offset—the time at which the car returns to the center of the third lane. The lane-departure event repeated 5–10 s after the "response offset of the preceding lane-departure event." In Figs. 2(b) and (c), the EEG data recorded 1-s before the "deviation onset" was served as the baseline period of the driver's physiological state inside the brain, and the time duration from "deviation onset" to "response onset" was defined as the RT to represent the driver's arousal state. When subjects were alert, their RT to the random drift was short, resulting in a small deviation from the center of the lane. When the subjects were drowsy, the RT and resulting lane deviation was long.

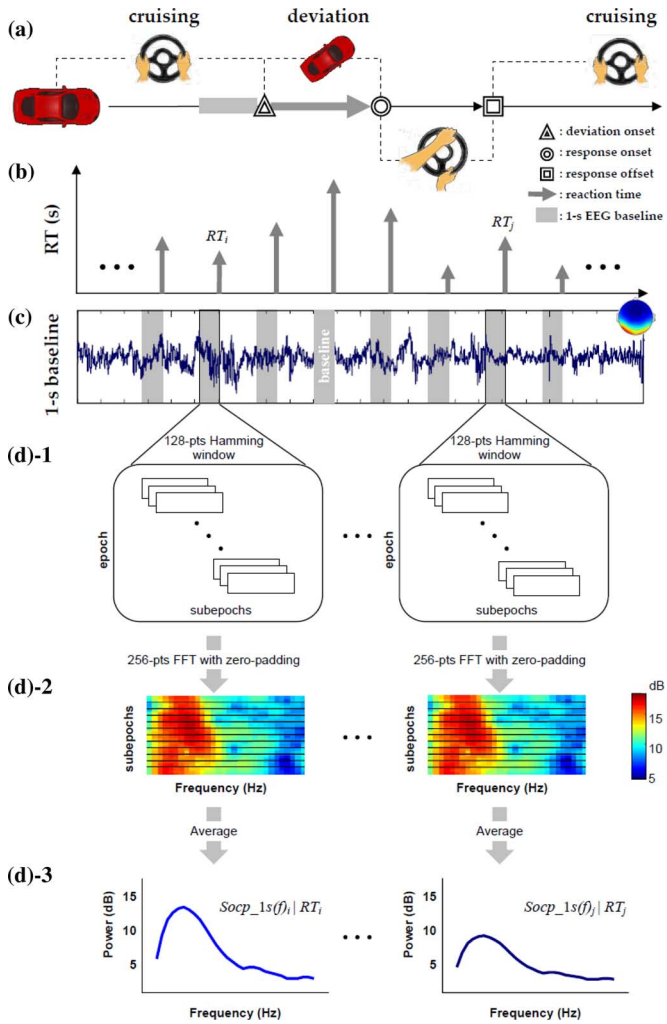

Fig. 2. (a) Event-related lane departure paradigm, (b) recoreded RT for all trials, (c) 1-s epoch EEG data of the occipital activation before the deviation onset (the baseline part during the cruising period), and (d) signal processing procedures of the spectral feature extraction including 128-pts Hamming window, 256-pts FFT, and zero-padding for each 1-s epoch. The output is a paired data set including the spectral power and the corresponding RT.

Based on this relationship between EEG and RT, we attempt to design a monitor system to process a 1-s EEG data continuously and to predict the RT for real-world applications.

C. Subjects and EEG Data Recording

The six volunteer subjects (aged 20 to 40 years) participated in the VR-based highway-driving experiments. All subjects involved in this study had good driving skills and were trained with the VR-based highway-driving for one day extra for familiarization before completing the testing section. Previous study [26] showed that people often become drowsy after one hour of continuous driving after lunch. These results indicate that drowsiness is not necessarily caused by long-hours driving. Hence, to maximize the chance of obtaining valuable data for this study, all the experiments were conducted in the early afternoon after lunch. On the first day, participants were instructed regarding the general procedures of the driving task. In addition, the participants completed an informed consent form. They

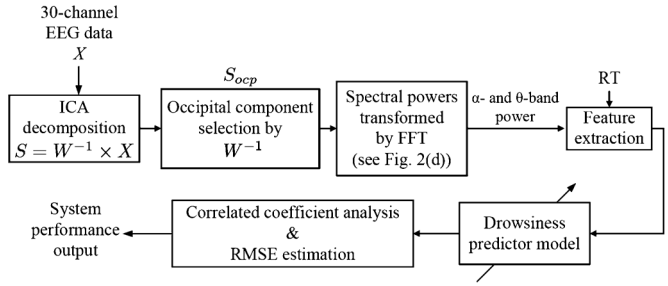

Fig. 3. Flowchart of the proposed drowsiness predictor, and the system performance is vertified by correlation coefficient analysis and RMSE of the recoreded RT and predicted RT.

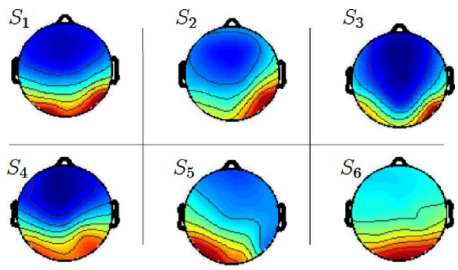

Fig. 4. The scalp topographies of the occipital component of six subjects.

began a 15- to 45-min practice session to learn how to keep the car in the center of the third cruising lane using the steering wheel. Participants were allowed to unlimited practice. On the test day, the participants were wired with an EEG cap. The EEG data acquisition process used 33 sintered Ag/AgCl EEG/EOG electrodes with a unipolar reference at right earlobe and 2 ECG channels with a bipolar connection placed on the chest. All the EEG/EOG electrodes were placed according to a modified International 10–20 system, and referred to the right ear lobe. Before data acquisition, the contact impedance between EEG electrodes and cortex was calibrated at less than 5 KΩ. A NeuroScan NuAmps Express system (Compumedics Ltd., VIC, Australia) simultaneously recorded the EEG/EOG/ECG data, lane deviations, and the RT. The EEG data was recorded with 16-bit quantization at a sampling rate of 500 Hz. Subsequent EEG data processing procedures employed 250 Hz down sampling to decrease the calculation load.

III. Data Analysis

In this study, the EEG data analysis and signal processing were implemented by scripts running in MATLAB (R2007a) and the EEGLAB Toolbox (ver. 5.03) developed by the Swartz Center for Computational Neruoscience, the University of California San Diego (UCSD) [27]. The flowchart of data processing procedures was illustrated in Fig. 3 that consists of Independent Component Analysis (ICA), power spectra analysis, feature extraction, drowsiness predictor model and correlation coefficient analysis and root mean square error (RMSE) for system performance estimation.

A. ICA

The blind source separation (BSS) problem [28], [29] deserves to be solved in the EEG signal which is usually con-

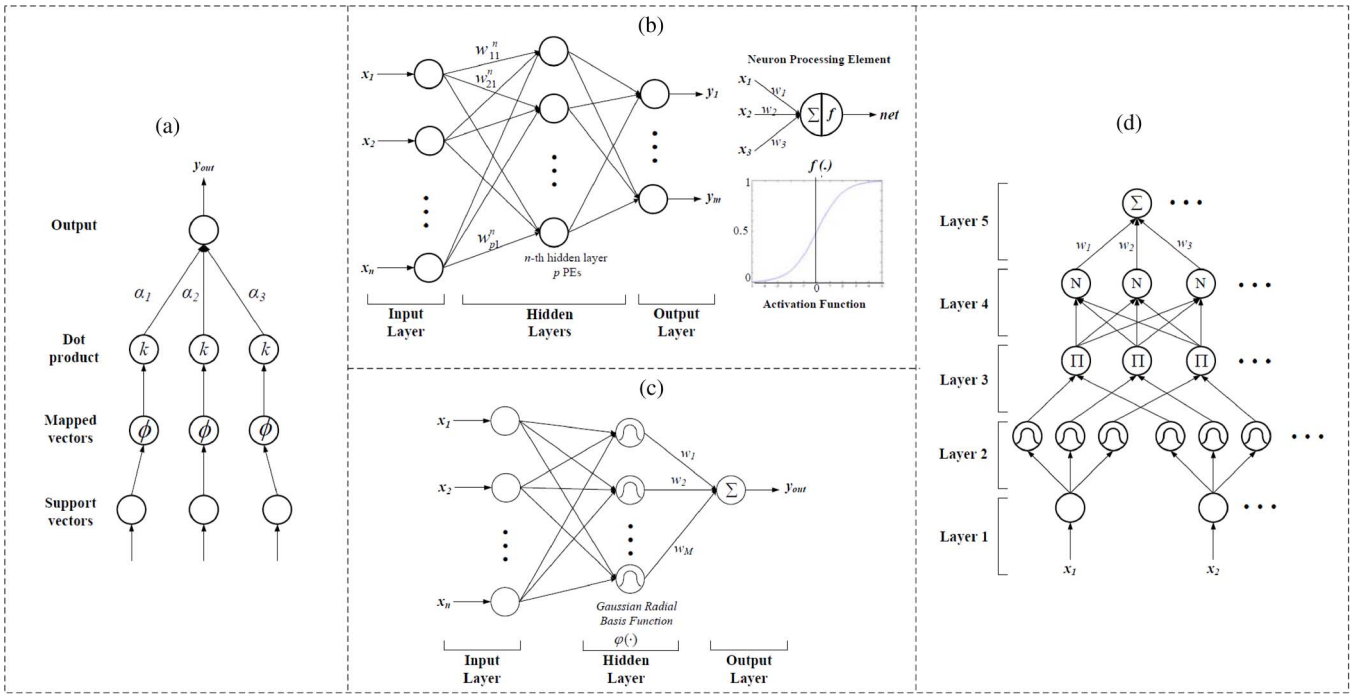

Fig. 5. Prediction models. Structure of the (a) SVR, (b) MLPNN, (c) RBFNN and (d) five-layer SONFIN.

taminated by various artifacts including eye movement and indoor power-line noise [30], [31]. One of the popular methods was applied ICA to find the linear projections that maximizes the mutual independences of estimated components. The general representation of ICA model can be simply denoted as $S = W^{-1} \times X$, where $S = [S_1, S_2, \ldots, S_n]^T$ presents the n independent sources, W^{-1} is the back-projection weighting matrix, and $X = [X_1, X_2, \ldots, X_n]^T$ is the n observed signals. The purpose of ICA algorithm is to find out the back-projection weighting matrix, W^{-1}, to have a maximum statistically independency of the separated components, S. Then, the occipital component [8]–[13], S_{ocp}, was selected by the weighting distribution of the scalp topography, which is rendered by W^{-1} [32], as the region of interest for power spectra analysis and feature extraction. The scalp topographies shown on Fig. 4 are the occipital component selected from six subjects.

B. Power Spectra Analysis and Feature Extraction

As shown in Fig. 3, the selected IC, S_{ocp}, related to occipital component were taken for power spectra analysis. In the first step of the spectral transformation, each 1-s length epoch (250 data points) was divided into several 128-point subepochs by Hanning windows. Then, we perform 256-point FFT with zero-padding for each subepoch to obtain the power spectral density. Finally, the average of spectral powers of subepochs was used for the spectral representation of this 1-s length occipital activation. Here, only the spectral powers of the θ-band (4–7 Hz) and α-band (8–12 Hz), which is reported as the significant index for the driving error [11], with the corresponding RT were used as the dataset pair to establish the prediction model.

C. Performance Estimation

To estimate the performance among different predictors, the Pearson Product-Moment Correlation Coefficient (PPMCC) and Root-Mean-of-Square-Error (RMSE) were applied in this study.

In this study, the PPMCC, denoted by r, between the estimated RTs and recorded RTs was obtained by

$$r = \frac{\sum_{i=1}^{n}(RT_i - \overline{RT})(eRT_i - \overline{eRT})}{\sqrt{\sum_{i=1}^{n}(RT_i - \overline{RT})^2}\sqrt{\sum_{i=1}^{n}(eRT_i - \overline{eRT})^2}} \quad (1)$$

where n is the number of trials. The $\overline{RT}$ and $\overline{eRT}$ are the average of recorded RTs and the estimated RTs, respectively. If r is high, it can be claimed that two variables have a strong linear relationship and the performance of the predictor is better [12], [18], [19].

The RMSE was another popular and useful index for assessing the performance of the predictor [33]. The RMSE could be estimated as the following:

$$RMSE = \frac{\sqrt{\sum_{i=1}^{n}(RT_i - eRT_i)^2}}{n} \quad (2)$$

where a smaller RMSE presents a better prediction for the proposed model.

IV. Drowsiness Prediction Models

This paper adopts four models for drowsiness prediction: (1) SVR, (2) MLPNN, (3) RBFNN, and (4) SONFIN. Here, all of the proposed approaches predict an unseen RT while confronting an unexpected event in terms of the spectral features of

TABLE I
OBSERVING LANE-DEPARTURE EVENT NUMBER FOR EACH SUBJECT

Subject	1	2	3	4	5	6	Total
Trials	335	335	228	224	236	236	1,594

TABLE II
CORRELATION COEFFICIENTS COMPARISONS FOR SUBJECT-DEPENDENT DROWSINESS PREDICTION

Subject		1	2	3	4	5	6	Average (%)
SVR	Training	96.1%	95.5%	97.3%	97.2%	97.1%	97.5%	96.8±2.1
	Testing	95.2%	95.5%	94.0%	93.7%	97.3%	95.7%	95.2±1.5
MLPNN	Training	94.6%	97.1%	95.7%	97.0%	96.9%	98.3%	96.6±3.9
	Testing	94.2%	97.1%	94.7%	96.7%	96.5%	98.2%	96.2±0.4
RBFNN	Training	95.6%	95.3%	92.8%	95.8%	95.9%	96.8%	95.4±1.8
	Testing	95.1%	95.7%	91.8%	93.6%	95.4%	97.3%	94.8±0.5
SONFIN	Training	95.6%	96.8%	96.6%	97.0%	97.4%	98.3%	96.7±1.5
	Testing	95.7%	97.4%	96.6%	97.3%	97.7%	98.8%	97.2±1.6

the occipital activation. The following section briefly describes the structure of each predictor.

A. SVR

The support vector machine is a popular approach for solving the problem of multidimensional function estimation and has been applied to various fields such as classification and regression. When SVM is employed dedicatedly for solving the problems of function approximation and regression estimation, it was denoted as the support vector regression (SVR). Fig. 5(a) shows the graphical overview for all steps. The SVR is a complicated and heavy-computation implementation of prediction algorithm based on structuring risk minimization principles to obtain a good generalization capability [34], [35]. For ε-SVR, it is formulated as minimization of the (3) as the following:

$$\min \frac{1}{2}\|\omega\|^2 + C\sum_{i}^{n}\left(\zeta_i + \zeta_i^*\right), \quad \text{subject to} \begin{cases} y_i - f(x_i,\omega) \le \varepsilon + \zeta_i^* \\ f(x_i,\omega) - y_i \le \varepsilon + \zeta_i \\ \zeta_i^*, \zeta_i \ge 0, \quad i = 1,\ldots,n \end{cases} \tag{3}$$

In this study, a library of LIBSVM [36] was used for SVR model construction with the radial basis function applied as its kernel function.

B. MLPNN

The MLPNN is the most commonly used neural-network architecture because of its capability to learn and generalize relatively small training-set requirements, fast operation, and ease of implementation [37], [38]. The MLPNN structure includes one input layer, one output layer, and a couple of hidden layers, as Fig. 5(b) shows.

For the n-layer, j-PE (processing element) output, y_j^n can be written as

$$y_j^n = f\left(net_j^n\right), \quad net_j^n = \sum_i w_{ji}^n y_i^{n-1} - b_j^n \tag{4}$$

where $f(.)$ is the activation function, w_{ji} is the weight from i-PE to j-PE and b_j denotes the bias value for net_j. The MLPNN estimates the weights to minimize the cost function using a back propagation-learning algorithm

$$E = \frac{1}{2}(d_k - y_k)^2. \tag{5}$$

The Gaussian activation function in (6) applies to all hidden layers, while the output layer uses a linear activation function

$$f(x) = \frac{1}{1+e^{-ax}}. \tag{6}$$

This study employs a 5-layer MLPNN with [10 6 5] processing elements (PEs) of hidden layers and 8-layer MLPNN with [10 6 5 4 3 2] PEs of hidden layers for subject-dependent and generalized cross-subject drowsiness prediction, respectively.

C. RBFNN

The radial basis function nerual network (RBFNN) is designed for (nonlinear) function approximation problem with a high-dimension space. The RBFNN provides a best fitting curve of the training data, and its implementation is much simpler than the perceptron approach while retaining the major property of universal approximation of functions [39]. The RBFNN is a 3-layer feed forward neural network structure that consists of an input layer, a single hidden layer with a nonlinear (Gaussian)

TABLE III
RMSE COMPARISONS FOR SUBJECT-DEPENDENT DROWSINESS PREDICTION

Subject		1	2	3	4	5	6	Average (s)
SVR	Training	0.084	0.083	0.093	0.087	0.088	0.093	0.088±0.038
	Testing	0.111	0.104	0.164	0.175	0.119	0.155	0.13±0.038
MLPNN	Training	0.075	0.054	0.095	0.095	0.071	0.056	0.089±0.025
	Testing	0.083	0.059	0.103	0.109	0.083	0.065	0.084±0.034
RBFNN	Training	0.067	0.070	0.125	0.112	0.088	0.077	0.074±0.030
	Testing	0.073	0.076	0.133	0.143	0.108	0.088	0.103±0.043
SONFIN	Training	0.068	0.057	0.085	0.094	0.069	0.055	0.071±0.020
	Testing	0.071	0.059	0.088	0.100	0.082	0.055	0.076±0.022

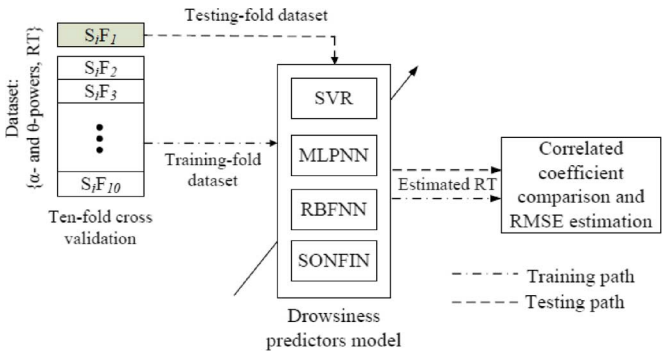

Fig. 6. Subject-dependent drowsiness predictor ten-fold cross-validation analysis structure, where S_iF_j means the j-th fold of the i-th subject.

RBF activation function and a linear output layer, as Fig. 5(c) shows.

The output y_{out} can be written as

$$y_{\text{out}} = \varphi(x) = \sum_{k=1}^{M} w_k \cdot e^{-\frac{\|x-c_k\|^2}{2(\sigma_k)^2}} \tag{7}$$

where w_k is the linear combinational weight, c_k is the center of the Gaussian RBF and σ_k is its variance. The Orthogonal Least-Squares (OLS) and gradient descent learning algorithms [40]–[45][52] were employed to minimize the error cost function

$$E(t) = \frac{1}{2}\left(y(t)_{\text{out}} - y_t\right)^2 = \left(\sum_{k=1}^{M} w_k(t) \cdot e^{-\frac{\|x-c_k\|^2}{2(\sigma_k)^2}} - y_t\right)^2. \tag{8}$$

The RBFNN employed 30–40 and 300–500 neurons for subject-dependent drowsiness prediction and generalized subject-independent drowsiness prediction, respectively.

D. SONFIN

The SONFIN [43] combines the nodes with a finite "fan-in" of connections represented by weight values from other nodes, and a "fan-out" of connections to other nodes. The integration function f combines information, activation, or evidence from other nodes, and is denoted as

$$net - input = f\left[u_1^k, u_2^k \ldots u_p^k, w_1^k, w_2^k \ldots w_p^k\right] \tag{9}$$

where $u_1^k, u_2^k, \ldots, u_p^k$ are inputs to this node, and $w_1^k, w_2^k, \ldots, w_p^k$ are the associated linking weights. The superscript $\{k\}$ in this equation indicates the layer number. The output for each node is an activation function value of its net input, $output = a(f)$, where $a(.)$ represents the activation function.

The functions of the nodes in each of the five layers of the SONFIN structure are briefly described as follow.

Layer1: Transmit inputs to the next node directly, without computation.

$$f = u_i^{(1)}, a^{(1)} = f. \tag{10}$$

Layer2: Calculate the output of Layer 1 into a fuzzy set.

$$f\left[u_{ij}^{(2)}\right] = -\frac{\left[u_i^{(2)} - m_{ij}\right]^2}{\sigma_{ij}^2}, a^{(2)} = e^f. \tag{11}$$

Layer3: Perform a fuzzy rule with an AND operation.

$$f\left[u_i^{(3)}\right] = \Pi u_i^{(3)} = e^{-[D_i(x-m_i)]^T[D_i(x-m_i)]}, a^{(3)} = f. \tag{12}$$

Layer4: Normalize the firing strength calculated in Layer 3.

$$f\left[u_i^{(4)}\right] = \sum_i u_i^{(4)}, a^{(4)}(f) = \frac{u_i^{(4)}}{f}. \tag{13}$$

Layer5: Integrate all the actions from Layer 5 to defuzzify the results. Each node in this layer corresponds to one output variable

$$f\left[u_i^{(5)}\right] = \sum_i w_i u_i^{(5)}, a^{(5)}(f) = f. \tag{14}$$

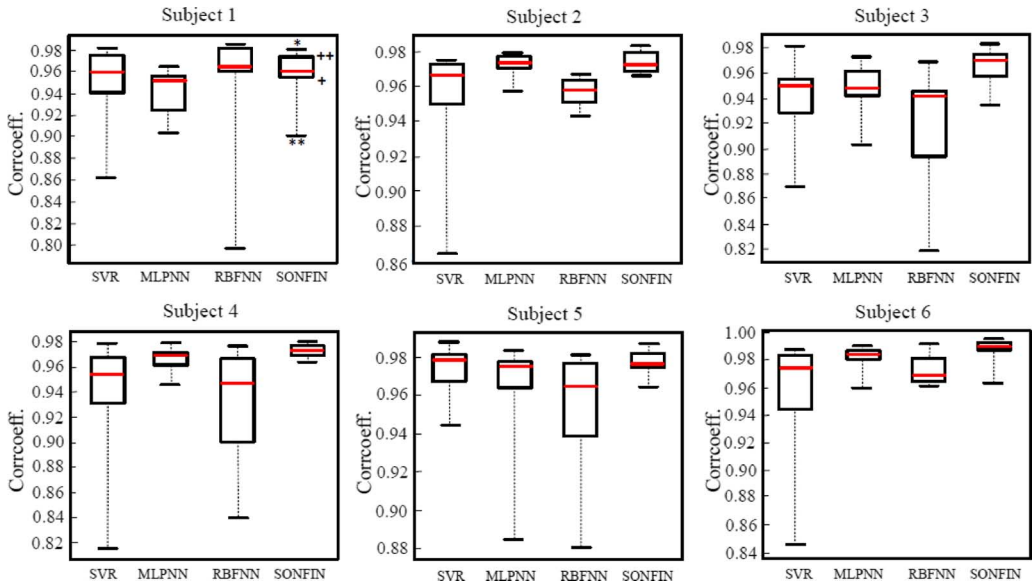

Fig. 7. Correlation coefficient boxplot comparison of subject's drowsy state testing evaluation for subject-dependent drowsiness prediction experiment with SVR, MLPNN, RBFNN and SONFIN. The boxes have three lines to present the values for lower quartile $(+)$, median (red line), and upper quartile $(++)$ for column data. Two addition lines at both ends of the whisker indicate the maximum $(*)$ and minimum $(**)$ value of a column data.

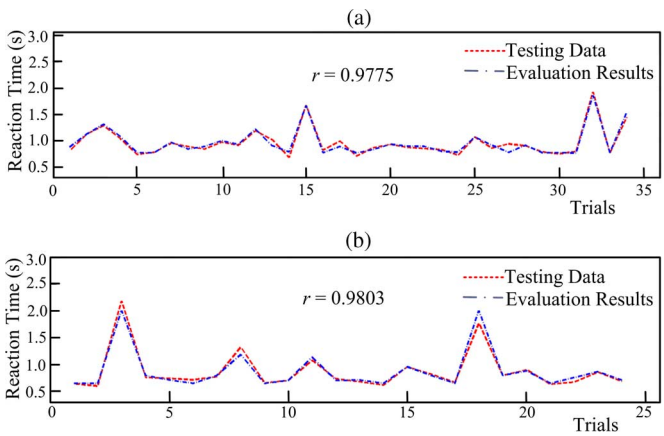

Fig. 8. Examples of testing data evaluation results of subject-dependent drowsiness prediction experiment with SONFIN for (a) subject 2 ($r = 0.9775$), and (b) subject 6 ($r = 0.9803$). The red dashed line and bule dashdot line present the golden testing data and estimated evaluatioin result respectively.

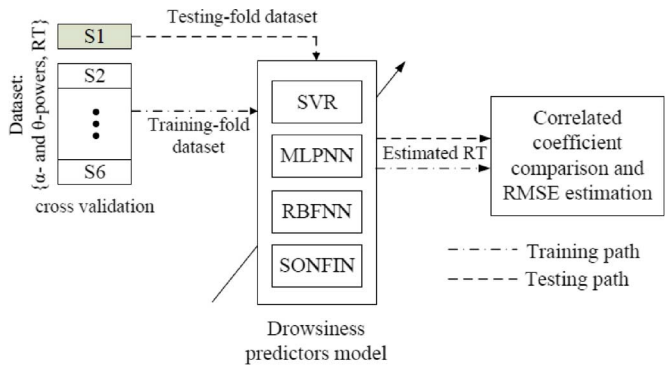

Fig. 9. Generalized cross-subject drowsiness predictor analysis structure, where S_i means the i-th subject.

The average rule numbers derived for subject-dependent drowsiness prediction and generalized cross-subject drowsiness prediction was less than 10.

V. Experimental Results and Discussion

In this study, a total of six normal healthy subjects participated in the VR-based highway-driving experiments described in Section II-A. The observing driving events of each subject are consisted of 224 to 335 lane-departure events and the EEG data length for subject 1 to 6 used for ICA decomposition are 44.7 min, 44.7 min, 30.4 min, 29.9 min, 31.5 min and 31.5 min. The occipital components from six subjects were selected the region of interest for establishing the prediction model. In total, we collected about 1594 trial samples as shown in Table I. The observing data are fed into FFT to transform into EEG power spectra, which are served as the inputs to the SVR, MLPNN, RBFNN and SOFIN predictors. This study applied two validation approaches to verify the performance and robustness of these predictors. The subject-dependent drowsiness prediction using ten-fold cross-validation was first utilized to evaluate the average single-subject performance. In this evaluation, 90% of the trials for each subject were used for training, while the remaining ten-percent of the trials were used for testing. The other validation approach is to evaluate the generalized cross-subject drowsiness prediction performance which was developed to be compared with the performance of the subject-dependent models. In the cross-subject drowsiness prediction regime, the EEG power spectra from randomly selected five subjects are used for training, and the remaining subject was used for testing samples.

A. Subject-Dependent Drowsiness Prediction

The performan This drowsiness-prediction procedure is depicted in Fig. 6. From statistical point of view, each subject completed a 10-round ten-fold cross-validation, in which 90% of

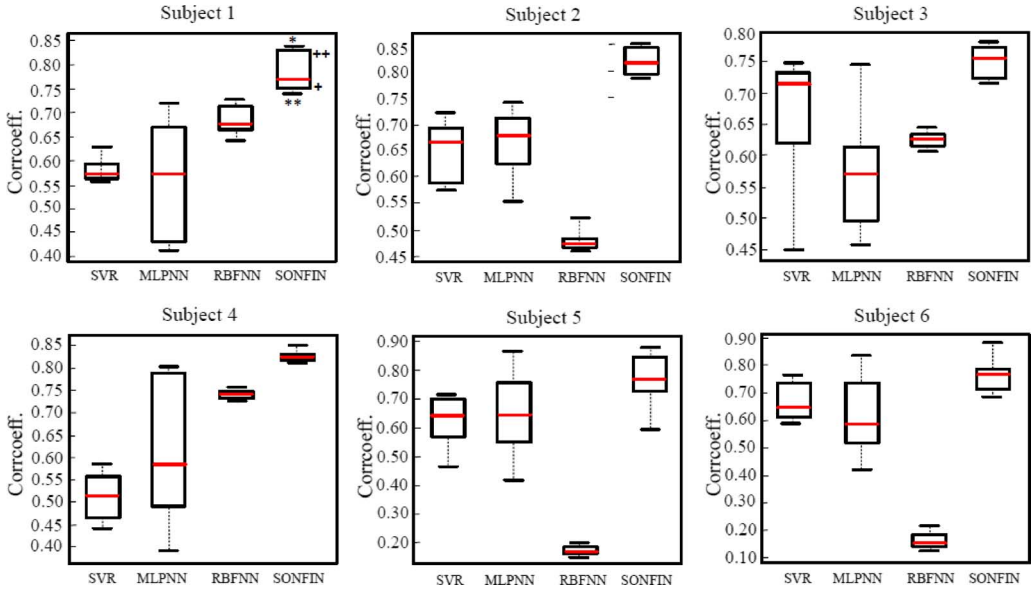

Fig. 10. Correlation coefficient boxplot comparison of subject's drowsy state testing evaluation for generalized cross-subject drowsiness prediction experiment with SVR, MLPNN, RBFNN and SONFIN. The boxes have three lines to present the values for lower quartile $(+)$, median (red line), and upper quartile $(++)$ for column data. Two addition lines at both ends of the whisker indicate the maximum $(*)$ and minimum $(**)$ value of a column data.

the trials were randomly selected as the training set and the reminding 10% of the trials as testing set The averages of PPMCC and RMSE between the actual and estimated RTs is shown on Tables II and III, respectively. The PPMCC on the training and testing sets obtained by SVR, MLPNN, RBFNN, and SONFIN are 96.8%, 96.6%, 95.4%, 96.7% and 95.2%, 96.2%, 94.8%, 97.2%, respectively The RMSE of training and testing data obtained by SVR, MLPNN, RBFNN, and SONFIN are 0.088 s, 0.089 s, 0.074 s, 0.071 s and 0.130 s, 0.084 s, 0.103 s, 0.076 s. Fig. 7 depicts the boxplot of the PPMCC of subject-dependent drowsiness prediction with 10-fold cross-validation using SVR, MLPNN, RBFNN and SONFIN. Take Subject 1 for example, the median, upper and lower quartile, maximum and minimum PPMCC for subject-dependent drowsy state predictor with SONFIN are 96.0%, 95.6% and 97.2%, 98.0% and 90.2%, respectively. Fig. 8 shows one sample result of RT estimations on the testing data with constructed SONFIN model for (a) subject 2 $(r = 97.6\%)$, and (b) subject 6 $(r = 98.0\%)$. The PPMCC of training data validation for subject 2 and subject 6 in the sample results depicted above are 96.3% and 98.5% respectively.

ces of all four predictors are comparable in subject-dependent drowsiness prediction, and SONFIN has a better PPMCC and a smaller RMSE value on testing data in this experiment ($r = 97.2\%$ and $\mathrm{RMSE} = 0.076$). However, subject-dependent prediction system is not applicable in real world to be generalized for other users. Developer must record user's EEG data in advance and only the recorded user can achieve that high performance $(r > 95\%)$. Therefore, a generalized cross-subject drowsiness prediction system shall be constructed.

B. Generalized Cross-Subject Drowsiness Prediction

The procedure of generalized cross-subject drowsiness predictor analysis is depicted in Fig. 9. The EEG data from five

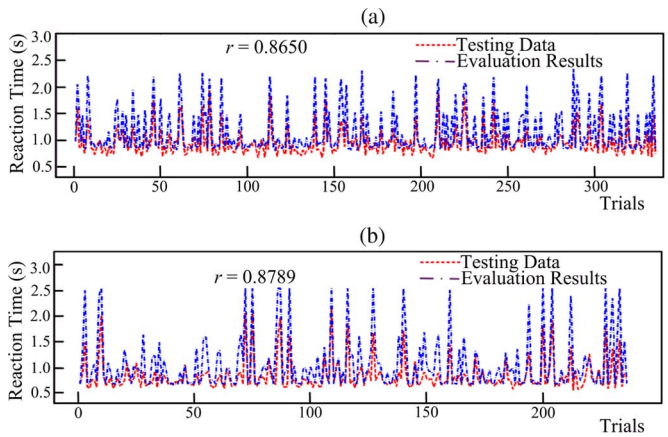

Fig. 11. Examples of testing data evaluation results of generalized cross-subject drowsiness prediction experimant with SONFIN for (a) subject 2 $(r = 0.8650)$, and (b) subject 6 $(r = 0.8789)$. The red dashed line and bule dashdot line present the golden testing data and estimated evaluatioin result respectively.

subjects were used as the training data, and the remaining subject was reserved as the testing pattern. Tables IV and V shows the averages of PPMCC and RMSE performance in comparison with the actual and estimated RTs. The PPMCC on the training and testing sets using obtained by SVR, MLPNN, RBFNN, and SONFIN are 98.0%, 96.8%, 99.3%, 98.4% and 61.6%, 61.3%, 47.9%, 78.3%, respectively. The RMSE values for training and testing evaluation with SVR, MLPNN, RBFNN, and SONFIN are 0.06 s, 0.04 s, 0.01 s, 0.06 s and 0.37 s, 0.42 s, 1.01 s, 0.36 s, respectively. Fig. 10 shows the boxplot of the PPMCC for cross-subject drowsiness prediction using SVR, MLPNN, RBFNN, and SONFIN. Take Subject 1 for example, the median, upper and lower quartile, maximum and minimum PPMCC for cross-subject drowsy state predictor with SONFIN are 77.0%, 82.9% and 74.6%, 84.0% and 74.5%, respectively. Fig. 11 shows one

TABLE IV
CORRELATION COEFFICIENTS COMPARISONS FOR GENERALIZED CROSS-SUBJECT DROWSINESS PREDICTION

Subject		1	2	3	4	5	6	Average (%)
SVR	Training	96.5%	99.1%	95.5%	98.8%	98.9%	99.0%	98.0±1.4
	Testing	58.0%	65.3%	66.4%	51.4%	62.2%	66.5%	61.6±8.6
MLPNN	Training	95.4%	99.4%	98.9%	91.6%	98.5%	97.0%	96.8±9.7
	Testing	56.5%	66.5%	58.2%	61.2%	63.8%	61.6%	61.3±12.2
RBFNN	Training	99.4%	99.6%	99.7%	98.7%	99.4%	98.7%	99.3±0.5
	Testing	68.3%	48.5%	62.6%	74.2%	17.1%	16.5%	47.9±23.6
SONFIN	Training	98.5%	99.1%	97.9%	97.6%	98.2%	99.0%	98.4±1.3
	Testing	78.1%	81.7%	74.6%	82.7%	76.0%	76.4%	78.3±5.7

sample result of RT estimations on the testing data with constructed SONFIN model for (a) subject 2 ($r = 86.5\%$), and (b) subject 6 ($r = 87.9\%$). The correlation coefficients of training data validation for subject 2 and subject 6 in the sample results depicted above are 99.3% and 98.6% respectively. Compared to the subject-dependent drowsiness results, the averaged PPMCC between the actual and estimated RTs on training data with these four predictors maintained sound results. However, the PPMCC obtained by the generalized cross-subject drowsiness prediction showed a significant performance decline on the test data (p-value <0.038). Only SONFIN still maintained a better PPMCC between actual and estimated RTs at 78.3% than other predictors. Furthermore, the SONFIN produced the lowest RMSE (0.36 s) on the testing data in this experiment. According to safety distance between vehicles reported by CEDR [44] and RSA [45], a rule thumb of 2-s braking distance under dry ground conditions with additional reaction distance of 18.3 m at a 100 km/hr car speed is recommended. The RMSE of proposed cross-subject drowsiness predictor with SONFIN is 0.36 s or 10 m at a 100 km/hr car speed in average, which does not violate the recommended reaction distance requirement of 18.3 m. Therefore, the proposed cross-subject drowsy state predictor with SONFIN showed a promising model for real-life applications.

C. Discussion

The reason for this drastic performance drop in generalized cross-subject drowsiness prediction using SVR, MLPNN, and RBFNN is that EEG data characteristics between distinct subjects usually vary widely. A model constructed by training data from individuals might not be generalized to others. Therefore, it is difficult to predict subject's behavior with others subjects' EEG without more adaptive features like SONFIN can provide. The SVR, MLPNN, and RBFNN provide a good system performance for subject-dependent drowsiness prediction due to the small power variation within the same subject. Fig. 12 demonstrates the 14 RT estimation rules automatically generated by generalized cross-subject drowsiness prediction with SONFIN.

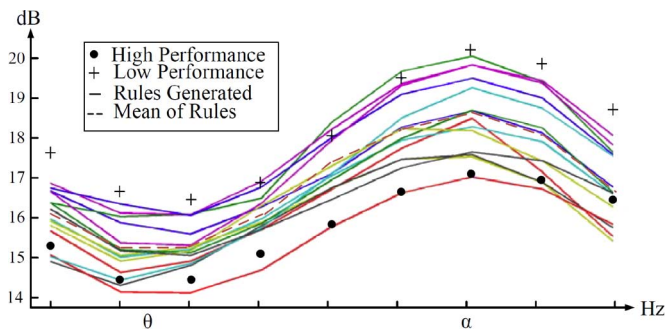

Fig. 12. One example of rules generated by SONFIN with generalized cross-subject drowsiness prediction.

The red dash line is the mean of these rules. Denote the rules triggered over this mean line is Low Performance (LP) rules, while the rules triggered below LP are denoted as High Performance (HP) rules. Two test samples with '+' (LP state) and '.' (HP state) sign were fed into this model, and the rules triggered here are mostly by LP and HP, respectively. This is the evidence engaging with the previous studies to use theta- and alpha-band for indexing the arousal state, and furthermore the derived fuzzy rules perform in the same manner with the trend of spectral powers.

VI. CONCLUSION

The amplitude of an EEG signal fluctuates on the microvolt level, making the EEG signal extremely noise-sensitive and easily influenced by artifacts. In addition, the EEG features between different subjects usually vary widely, making it difficult to apply and generalize results from one individual to another. The proposed EEG signal-processing procedures and SONFIN method in this study overcome these two limitations. Signal-processing methods based on ICA and time-frequency analysis successfully excludes the EEG contaminations and extracts the EEG features related to task performance. For each experiment, 1-s baseline theta- and alpha-band power spectra of the activations of the occipital component, along with RTs

TABLE V
RMSE COMPARISONS FOR GENERALIZED CROSS-SUBJECT DROWSINESS PREDICTION

Subject		1	2	3	4	5	6	Average (s)
SVR	Training	0.092	0.046	0.089	0.049	0.048	0.047	0.060±0.030
	Testing	0.222	0.309	0.454	0.267	0.540	0.337	0.370±0.110
MLPNN	Training	0.069	0.025	0.024	0.060	0.033	0.041	0.040±0.070
	Testing	0.229	0.448	0.578	0.366	0.443	0.430	0.420±0.150
RBFNN	Training	0.006	0.006	0.006	0.003	0.005	0.004	0.010±0.002
	Testing	0.417	0.467	0.798	3.361	0.496	0.507	1.010±1.070
SONFIN	Training	0.058	0.048	0.060	0.063	0.060	0.046	0.060±0.020
	Testing	0.153	0.318	0.537	0.371	0.321	0.488	0.360±0.140

of trials, were used to build an RT prediction model. This study tests four predictors, SVR, MLPNN, RBFNN, and SONFIN, for drowsiness prediction. Experimental results of this study showed that it is feasible to estimate subject's reaction times based on 1-s EEG power spectra before the onsets of lane-departure events. A comparison between subject-dependent and cross-subject prediction models showed that the subject's RTs could be better estimated by an individualized RT prediction model. Furthermore, SONFIN outperformed SVR, MLPNN, and RBFNN in terms of PPMCC and RMSE especially for the cross-subject case. This demonstration might lead to a practical system for noninvasive predicting and monitoring subject responses to critical events in real-world applications. However, some notifications and limitations shall be highlighted here before applying proposed system to a practical environment. The proposed SONFIN system shall be applied only to the environments that are not dangerous even if an operation error occurs. It can be implemented just as a passive and assistive alert system to warn the driver if he/she is becoming excessively drowsy and could fall asleep while driving.

ACKNOWLEDGMENT

The views and the conclusions contained in this document are those of the authors and should not be interpreted as representing the official policies, either expressed or implied, of the Army Research Laboratory or the U.S Government. The U.S Government is authorized to reproduce and distribute reprints for Government purposes notwithstanding any copyright notation herein.

REFERENCES

[1] US National Sleep Foundation, "1.9 Million Drivers Have Fatigue-Related Car Crashes or Near Misses Each Year," Nov. 2009 [Online]. Available: http://www.sleepfoundation.org/article/press-release/19-million-drivers-have-fatigue-related-car-crashes-or-near-misses-each-year

[2] K. Kozak, J. Pohl, W. Birk, J. Greenberg, B. Artz, M. Blommer, L. Cathey, and R. Curry, "Evaluation of lane departure warnings for drowsy drivers," in *Proc. Human Factors and Ergonomics Society 50th Annual Meeting*, Oct. 16–20, 2006, pp. 2400–2404.

[3] M. Rimini-Doering, T. Altmueller, and U. Ladstaetter, "Effects of lane departure warning on drowsy drivers' performance and state in a simulator," in *Proc. 3rd Int. Driving Symp. Human Factors in Driver Assessment, Training Veh. Design*, Rockport, ME, Jun. 27–30, 2005, pp. 88–95.

[4] J. C. Popieul, P. Simon, and P. Loslever, "Using driver's head movements evolution as a drowsiness indicator," in *Proc IEEE Intell. Veh. Symp.*, 2003, pp. 616–621.

[5] Q. Ji, Z. Zhu, and P. Lan, "Real-time nonintrusive monitoring and prediction of driver fatigue," *IEEE Trans. Veh. Technol.*, vol. 53, no. 4, pp. 1052–068, Jul. 2004.

[6] D. K. McGregor and J. A. Stern, "Time on task and blink effects on saccade duration," *Ergonomics*, vol. 39, no. 4, pp. 649–660, Mar. 1996.

[7] F. Zhang, A. Mishra, A. G. Richardson, and B. Otis, "A low-power ECoG/EEG processing IC with integrated multiband energy extractor," *IEEE Trans. Circuits Syst. I, Reg. Papers*, 2011, (ID: 10.1109/TCSI.2011.2163972).

[8] J. Beatty, A. Greenberg, W. P. Deibler, and J. F. O'hanlon, "Operant control of occipital theta rhythm affects performance in a radar monitoring task," *Science*, vol. 183, no. 4127, pp. 871–873, Mar. 1974.

[9] R. S. Huang, T. P. Jung, A. Delorme, and S. Makeig, "Tonic and phasic electroencephalographic dynamics during continuous compensatory tracking," *NeuroImage*, vol. 39, no. 4, pp. 1896–1909, Feb. 2008.

[10] R. S. Huang, T. P. Jung, and S. Makeig, "Tonic changes in EEG power spectra during simulated driving," *Lecture Notes in Computer Science*, vol. 5638, LNAI, pp. 394–403, Dec. 2009.

[11] C. T. Lin, R. C. Wu, S. F. Liang, W. H. Chao, Y. J. Chen, and T. P. Jung, "EEG-based drowsiness estimation for safety driving using independent component analysis," *IEEE Trans. Circuits Syst. I, Reg. Papers*, vol. 52, no. 12, pp. 2726–2738, Dec. 12, 2005.

[12] W. Klimesch, "EEG alpha and theta oscillations reflect cognitive and memory performance: A review and analysis," *Brain Res. Rev.*, vol. 29, no. 2–3, pp. 169–195, 1999.

[13] S. Makeig and T.-P. Jung, "Tonic, phasic, and transient EEG correlates auditory awareness in drowsiness," *Cognitive Brain Res.*, vol. 4, no. 1, pp. 15–25, 1996.

[14] M. A. Schier, "Changes in EEG alpha power during simulated driving: A demonstration," *Int. J. Psychophysiol.*, vol. 37, no. 2, pp. 155–162, 2000.

[15] C. T. Lin, Y. C. Chen, T. Y. Huang, T. T. Chiu, L. W. Ko, S. F. Liang, H. Y. Hsieh, S. H. Hsu, and J. R. Duann, "Development of wireless brain computer interface with embedded multitask scheduling and its application on real-time driver's drowsiness detection and warning," *IEEE Trans. Biomed. Eng.*, vol. 55, no. 5, pp. 1582–1591, May 2008.

[16] C. T. Lin, L. W. Ko, J. C. Chiou, J. R. Duann, R. S. Huang, S. F. Liang, T. W. Chiu, and T. P. Jung, "Noninvasive neural prostheses using mobile and wireless EEG," *Proc. IEEE*, vol. 96, no. 7, pp. 1167–1183, Jul. 2008.

[17] C. T. Lin, L. W. Ko, I. F. Chung, T. Y. Huang, Y. C. Chen, T. P. Jung, and S. F. Liang, "Adaptive EEG-based alertness estimation system by using ICA-based fuzzy neural networks," *IEEE Trans. Circuits Syst. I, Reg. Papers*, vol. 53, no. 11, pp. 2469–2476, Nov. 2006.
[18] C. T. Lin, R. C. Wu, T.-P. Jung, S.-F. Liang, and T. Y. Huang, "Estimating driving performance based on EEG spectrum analysis," *EURASIP J. Appl. Signal Process.*, vol. 2005, no. 19, pp. 3165–3174, 2005.
[19] F. C. Lin, L. W. Ko, S. A. Chen, C. F. Chen, and C. T. Lin, "EEG-based cognitive state monitoring and prediction by using the self-constructing neural fuzzy system," in *Proc. 2010 IEEE Int. Symp. Circuits Syst. (ISCAS 2010)*, Paris, France, 2010.
[20] A. Subasi, "Automatic recognition of alertness level from EEG by using neural network and wavelet coefficients," *Expert Syst. With Appl.*, vol. 28, no. 4, pp. 701–711, May 2005.
[21] M. K. Kiymik, M. Akin, and A. Subasi, "Automatic recognition of alertness level by using wavelet transform and artificial neural network," *J. Neurosci. Meth.*, vol. 139, no. 2, pp. 231–240, Oct. 2004.
[22] A. Vuckovic, V. Radivojevic, A. C. N. Chen, and D. Popovic, "Automatic recognition of alertness and drowsiness from EEG by an artificial neural network," *Med. Eng. Phys.*, vol. 24, no. 5, pp. 349–360, Jun. 2002.
[23] D. Stewart, "A platform with six degrees of freedom," *Proc. Inst. Mech. Eng.*, vol. 180, no. 5, pt. 1, pp. 371–386, 1965–1966.
[24] K. Liu, J. M. Fitzgerald, and F. L. Lewis, "Kinematic analysis of a Stewart platform manipulator," *IEEE Trans. Ind. Electron.*, vol. 40, no. 2, pp. 282–293, 1993.
[25] C. T. Lin, J. Y. Lin, and Y. C. Lin, "A neural fuzzy inference network for the motion analyses of Stewart platform," *Int. J. Fuzzy Syst.*, vol. 4, no. 2, pp. 704–714, 2002.
[26] H. Ueno, M. Kaneda, and M. Tsukino, "Development of drowsiness detection system," in *Proc. Veh. Navigation Inf. Syst. Conf.*, Aug. 1994, pp. 15–20.
[27] A. Delorme and S. Makeig, "EEGLAB: An open source toolbox for analysis of single-trial EEG dynamics including Independent Component Analysis," *J. Neurosci. Meth.*, vol. 134, no. 1, pp. 9–12, Mar. 2004.
[28] T. W. Lee, *Independent Component Analysis: Theory and Applications*. Norwell, MA: Kluwer, 1998.
[29] S. Javidi, D. P. Mandic, and A. Cichocki, "Complex blind source extraction from noisy mixtures using second-order statistics," *IEEE Trans. Circuits Syst. I, Reg. Papers*, vol. 57, no. 7, pp. 1404–1416, Jul. 2010.
[30] Z. Xue, J. Li, S. Li, and B. Wan, "Using ICA to remove eye blink and power line artifacts in EEG," in *Proc. 1st Int. Conf. Innovative Computing, Information Contr.*, 2006, vol. 3, pp. 107–110.
[31] T. P. Jung, S. Makeig, C. Humphries, T. W. Lee, M. J. McKeown, V. Iragui, and T. J. Sejnowski, "Removing electroencephalographic artifacts by blind source separation," *Psychophysiol.*, vol. 37, pp. 163–178, 2000.
[32] J. Onton, M. Westerfield, J. Townsend, and S. Makeig, "Imaging human EEG dynamics using independent component analysis," *Methodolog. Conceptual Adv. Study of Brain-Behavior Dynamics: A Multivariate Lifespan Perspective*, vol. 30, pp. 808–822, 2006.
[33] M. Shen, L. Lin, J. Chen, and C. Q. Chang, "A prediction approach for multichannel EEG signals modeling using local wavelet SVM," *IEEE Trans. Instrum. Meas.*, vol. 59, no. 5, pp. 1485–1492, May 2010.
[34] A. Alenezi, S. A. Moses, and T. B. Trafalis, "Real-time prediction of order flowtimes using support vector regression," *Computers & Operations Research*, vol. 35, no. ll, pp. 3489–3503, 2008.
[35] U. Thissen, M. Pepers, B. UstUn, W. J. Melssen, and L. M. C. Buydens, "Comparing support vector machines to PLS for spectral regression applications," *Chemometrics Intell. Lab. Syst.*, vol. 73, no. 2, pp. 169–179, 2004.
[36] C. C. Chang and C. J. Lin, "LIBSVM: A library for support vector machines," *ACM Trans. Intell. Syst. Technol.* vol. 2, pp. 27:1–27:27, 2011 [Online]. Available: http://www.csie.ntu.edu.tw/~cjlin/libsvm
[37] B. B. Chaudhuri and U. Bhattacharya, "Efficient training and improved performance of multilayer perceptron in pattern classification," *Neurocomput.*, vol. 34, pp. 11–27, 2000.
[38] I. Guler and E. D. Ubeyli, "Multiclass support vector machines for EEG-signals classification," *IEEE Trans. Info. Tech. Biomed.*, vol. 11, no. 2, pp. 117–126, Mar. 2007.
[39] S. Haykin, *Neural Networks: A Comprehensive Foundation*, 2nd ed. Upper Saddle River, NJ: Prentice Hall, 1999.
[40] L. X. Wang and J. M. Mendel, "Fuzzy basis functions, universal approximation, and orthogonal least-squares learning," *IEEE Trans. Neural Netw.*, vol. 3, pp. 807–814, Sep. 1992.
[41] L. X. Wang, *Adaptive Fuzzy Systems and Control*. Englewood Cliffs, NJ: Prentice-Hall, 1994.
[42] M. D. Buhmann, *Radial Basis Functions: Theory and Implementations*. Cambridge, U.K.: Cambridge Univ., 2003.
[43] C. F. Juang and C. T. Lin, "An online self-constructing neural fuzzy inference network and its applications," *IEEE Trans. Fuzzy Syst.*, vol. 6, no. 1, pp. 12–32, Feb. 1998.
[44] Conference of European Directors of Roads, Distance Between Vehicles May 2011 [Online]. Available: http://www.cedr.fr/home/index.php?id=218/e_Distance_between_vehicles.pdf
[45] Road Safety of Authority, Stopping Distances for Cars [Online]. Available: http://www.rulesoftheroad.ie/rules-for-driving/speed-limits/speed-limits_stopping-distances-cars.html

Fu-Chang Lin received the B.S. and M.S. degrees in electrical engineering from National Cheng-Kung University, Tainan, Taiwan, in 1995 and 1997, respectively. He is currently a Senior Application Constant in Synopsys Taiwan Limited and also working toward the Ph.D. degree at the National Chiao Tung University, Hsinchu, Taiwan.

His current research interests include artificial neural networks and biomedical signal processing.

Li-Wei Ko received the B.S. degree in mathematics from National Chung Cheng University, Taiwan, in 2001, the M.S. degree in educational measurement and statistics from National Taichung University in 2004, and the Ph.D. degrees in electrical engineering from National Chiao Tung University (NCTU), Taiwan, in 2007.

He is currently an Executive Officer of the Brain Research Center (BRC), and an assistant researcher/professor in Department of Biological Science and Technology in NCTU. He is also the visiting scholar at Institute for Neural Computation in University of California, San Diego. His primary research interests are to apply computational intelligence technologies such as time-frequency analysis and neural networks to analyze neural activities associated with human cognitive functions and develop the mobile and wireless brain machine interface in unconstrained, actively engaged human subjects in daily life applications. He recently is also involved in developing the intelligent and real time expert system in mobile and wireless healthcare such as the early detection system for cardiology disease patients and portable sleep stage monitoring system for sleep disorders in home. Relevant research fields cover neural networks, neural fuzzy systems, machine learning, brain computer interface, and computational neuroscience.

Dr. Ko currently is an IEEE Member and an Associate Editor of IEEE TRANSACTIONS ON NEURAL NETWORKS in IEEE Computational Intelligence Society (CIS). He is also involved in the Neural Network Technical Committee (NNTC) and reviewers of IEEE Journals, *Biomedical Signal Processing & Control*, and *Organization for Human Brain Mapping*.

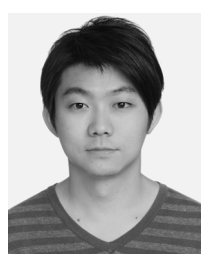

Chun-Hsiang Chuang received the B.S. degree from Taipei Municipal Teachers College, Taipei, Taiwan, in 2004, and the M.S. degree from the National Taichung University, Taichung, Taiwan, in 2009. He is currently working toward a Ph.D. degree at the Institute of Electrical and Control Engineering, National Chiao Tung University (NCTU), Hsinchu, Taiwan.

His research interests include machine learning and biomedical signal processing.

Tung-Ping Su received the B.S. degree in medicine from National Defense Medical Center (NDMC), Taiwan, in 1971.

He is currently the Vice Superintendent of Taipei Veterans General Hospital and the Professor of Medicine in National Yang-Ming University. He is also the President of Taiwanese Society of Biological Psychiatry and Neuropsychopharmacology (TSBPN). His research areas include: Schizophrenia and Affective disorders, Post-Traumatic Stress Disorder (PTSD), sleep disorders, neuroendocrinology, brain imaging, psychopharmacology, and pharmacoepidemiology.

Chin-Teng Lin received the B.S. degree from National Chiao-Tung University (NCTU), Taiwan, in 1986, and the M.S. and Ph.D. degrees in electrical engineering from Purdue University, West Lafayette, IN, in 1989 and 1992, respectively.

He is currently the Provost, Chair Professor of Electrical and Computer Engineering, and Director of Brain Research Center, National Chiao Tung University. He has published more than 120 journal papers in the areas of neural networks, fuzzy systems, multimedia hardware/software, and cognitive neuro-engineering, including approximately 74 IEEE journal papers.

Dr. Lin was elevated to be an IEEE Fellow for his contributions to biologically inspired information systems in 2005. He is elected as the Editor-in-chief of IEEE TRANSACTIONS ON FUZZY SYSTEMS. He also served on the Board of Governors at IEEE Circuits and Systems (CAS) Society in 2005–2008, IEEE Systems, Man, Cybernetics (SMC) Society in 2003–2005, IEEE Computational Intelligence Society in 2008–2010, and Chair of IEEE Taipei Section in 2009–2010. Dr. Lin was the Distinguished Lecturer of IEEE CAS Society from 2003 to 2005. He served as the Deputy Editor-in-Chief of IEEE TRANSACTIONS ON CIRCUITS AND SYSTEMS-II in 2006–2008. Dr. Lin was the Program Chair of IEEE International Conference on Systems, Man, and Cybernetics in 2005. Dr. Lin is the coauthor of Neural Fuzzy Systems (Prentice-Hall), and the author of Neural Fuzzy Control Systems with Structure and Parameter Learning (World Scientific).